Geochemical Perspectives Letters

Geobarometric evidence for a LM/TZ origin of $CaSiO_3$ in a sublithospheric diamond

P.-T. Genzel[1*], M.G. Pamato[2], D. Novella[2], L. Santello[2], S. Lorenzon[2], S.B. Shirey[3], D.G. Pearson[4], F. Nestola[2], F.E. Brenker[1]

https://doi.org/10.7185/geochemlet.2313

Abstract

Breyite is the second most abundant mineral inclusion in super-deep diamonds after ferropericlase. Though breyite stability extends to 300 km along typical mantle geotherm, this phase is often assumed to be the product of retrograde transformation of $CaSiO_3$-perovskite, and thus has the potential to retain information from as deep as 800–1000 km. In this study, we determined the depth of formation of a breyite inclusion still enclosed in its host diamond from Juína, Brazil, by X-ray diffraction. The measured >5 % smaller unit cell for breyite indicates a stored residual pressure showing that the breyite was entrapped between about 9(1) and 10(1) GPa. These are the highest estimates of formation pressure ever determined for a breyite inclusion. For ambient mantle temperatures higher than 1400–1500 °C, these pressures would exceed the maximum *P* of the breyite stability field. Breyite in this diamond cannot be primary but is rather a back-transformation product from $CaSiO_3$-perovskite formed in the transition zone or the lower mantle. The co-existence magnesite in diamond JU55 and the slab-association of sublithospheric diamonds is evidence of carbon transport to lower mantle depths.

Received 26 August 2022 | Accepted 31 March 2023 | Published 25 April 2023

Introduction

Diamond and its entrapped mineral inclusions represent the deepest natural materials from Earth's interior. The stability field for diamond in Earth, determined by laboratory experiments, ranges from about 150 km down to a depth of 2900 km (Maeda *et al.*, 2017). Diamond often encloses surrounding mantle minerals during growth (*e.g.*, Stachel, 2001; Brenker *et al.*, 2007; Stachel and Harris, 2009; Bulanova *et al.*, 2010), providing an exceptional window into the Earth's deep interior. A rare category of diamonds (Stachel and Harris, 2008), the so-called super-deep diamonds (or sublithospheric diamonds), are interpreted to crystallise between 300 km and a minimum of 800 km depth (Harte, 2010). This interpretation is based on mineral phases found as inclusions in these diamonds, although some are thought to be products of retrograde transformations from the transition zone or lower mantle precursors (*e.g.*, Shirey *et al.*, 2013).

The Earth's lower mantle mainly consists of ~75–80 % bridgmanite (~$MgSiO_3$), 10–15 % ferropericlase [(Mg,Fe)O], and 5–10 % of a $CaSiO_3$-phase with perovskite structure (*e.g.*, Harte, 2010). If these phases become trapped inside a diamond during its growth, they can be transported to the Earth's surface without reacting kimberlite magma or ambient mantle material (*e.g.*, Brenker *et al.*, 2021). During ascent, the inclusions remain chemically pristine but often transform to their lower-pressure polymorphs. However, in all other cases reported so far, a direct pressure determination that breyite (formerly called $CaSiO_3$-walstromite) formed at lower-pressure after $CaSiO_3$-perovskite has not been possible. After ferropericlase, breyite is the second most abundant (Brenker *et al.*, 2021) and the dominant Ca-bearing mineral found in super-deep diamonds (Joswig *et al.*, 1999). The $CaSiO_3$-phases are amenable to hosting elements such as Nd, Sr, U and Pb that allow radiometric dating and tracer isotopic studies. Therefore, constraining the ultimate depth of origin of $CaSiO_3$-inclusions is critical to understanding the geochemical information coming from these studies.

When breyite is simply considered to be the product of back-transformation from $CaSiO_3$-perovskite, it would be derived from a high-pressure assemblage of peridotitic/eclogitic mantle rocks at depths below 520 km (Kaminsky, 2012; Anzolini *et al.*, 2018). However, there are indications that breyite can also be a primary inclusion phase originating from much shallower depths within the upper mantle (Anzolini *et al.*, 2016; Thomson *et al.*, 2016). Recently, Brenker *et al.* (2021) summarised possible formation scenarios for breyite that do not necessarily require

1. Geoscience Institute, Goethe University Frankfurt, Altenhöferallee 1, 60438 Frankfurt am Main, Germany
2. Department of Geosciences, University of Padova, Via G. Gradenigo 6, 35131 Padova, Italy
3. Earth and Planets Laboratory, Carnegie Institution for Science, 5241 Broad Branch Rd NW, Washington, D.C. 20015, USA
4. Department of Earth and Atmospheric Sciences, University of Alberta, 1-26 Earth Sciences Building, Edmonton, Alberta T6G 2E3, Canada
* Corresponding author (email: genzel@em.uni-frankfurt.de)

great depths and showed that breyite formation is possible within the upper mantle as well. Thus, the abundance of breyite as an inclusion in sublithospheric diamonds makes determining its primary or retrograde mineral history essential in understanding mantle dynamics.

Breyite formation *via* exsolution from a $CaSiO_3$-$CaTiO_3$-perovskite solid solution only requires pressures below 10 GPa, corresponding to depths of 270–300 km within the upper mantle, shown experimentally (Kubo *et al.*, 1997) and through natural intergrowths between the two phases (*e.g.*, Bulanova *et al.*, 2010; Zedgenizov *et al.*, 2016). Further, breyite can form as a product of the retrograde reaction of larnite (β-Ca_2SiO_4) and titanite-structured $CaSi_2O_5$ at pressures between 9 and 10 GPa at depths not greater than 270–300 km (Brenker *et al.*, 2005; Anzolini *et al.*, 2016, 2018). The reaction of carbonate and a Si-rich component can also lead to breyite formation (Brenker *et al.*, 2005, 2007). For this last scenario, two different pressure estimates were postulated: one at very low pressures of about 6 GPa or less (Fedoraeva *et al.*, 2019) under SiO_2-poor conditions, and another at a maximum pressure of about 6–8 GPa (Woodland *et al.*, 2020) in SiO_2-enriched environments.

These different formation mechanisms show that the sole occurrence of breyite in a diamond cannot be used as a stand-alone criterion to propose its depth of origin (Brenker *et al.*, 2021) without other independent geobarometric determinations. It is known that diamond retains a certain pressure on its inclusions, known as “residual pressure” P_{inc} (or internal pressure) (see Supplementary Information; Angel *et al.*, 2022). By determining the residual pressure of an inclusion by single-inclusion elastic geobarometry, a minimum pressure for a given

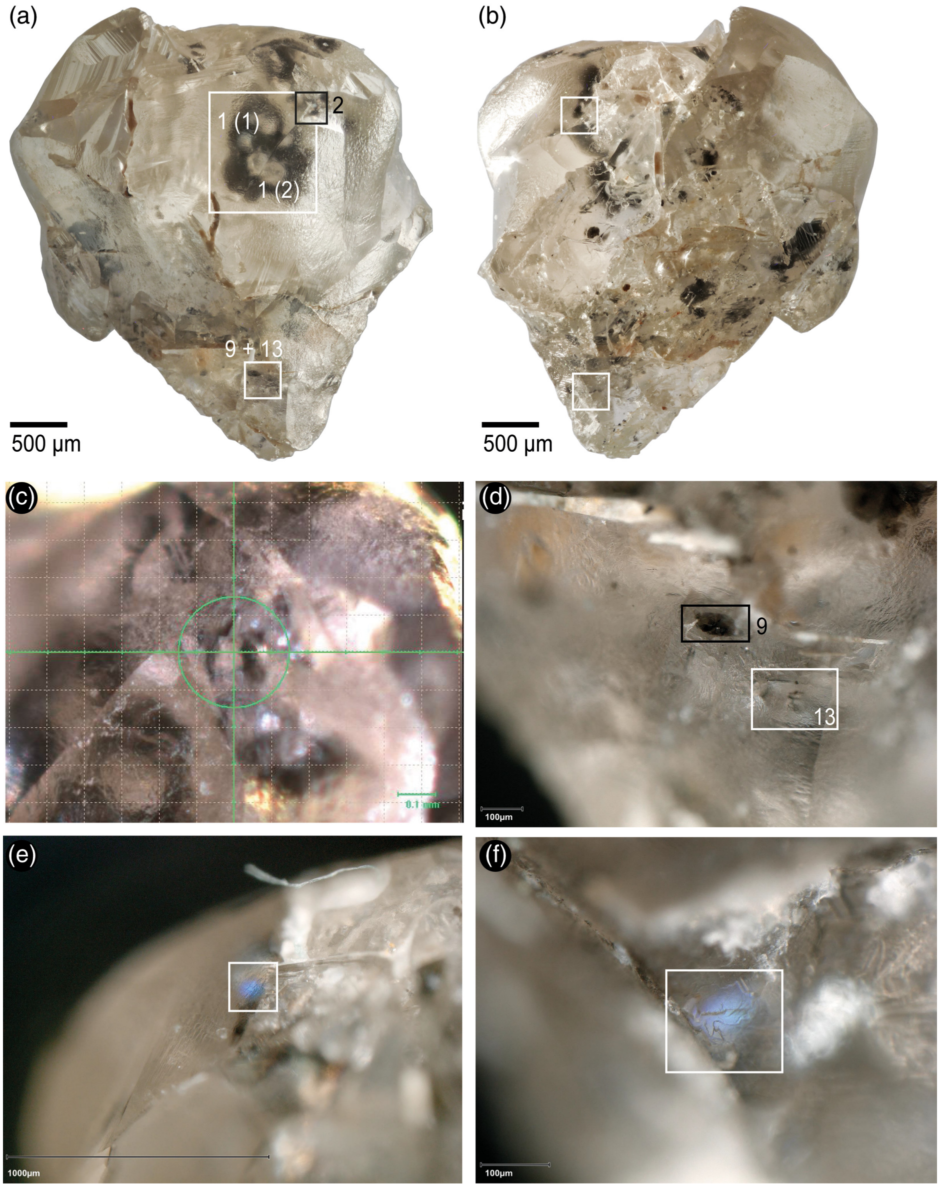

Figure 1 **(a)** Overview of the front of diamond JU55 of this work. The black square shows the location of the breyite inclusion 2, while the larger white square shows two groups of colourless breyite inclusions, groups 1(1) and 1(2). The white square shows inclusions 9 and 13, resulted to be the two TiO_2 polymorphs (inclusion 9) rutile and anatase, and magnesite (inclusion 13). **(b)** Overview of the back of diamond JU55. The white squares show the locations of the ferropericlase inclusions. **(c)** Detailed view of the breyite inclusion 2. **(d)** Detailed view of inclusion 9 (black square) and 13 (white square). **(e)** Detailed view of the first ferropericlase inclusion. **(f)** Detailed view of the second ferropericlase inclusion.

temperature of the entrapment of a mineral inclusion in its host diamond can be calculated (Angel *et al.*, 2014, 2015). The presence of fractures and/or cracks around the inclusions can affect and decrease the residual pressure as discussed in detail by Angel *et al.* (2022).

A very reliable way to measure P_{inc} is by X-ray diffraction getting the unit-cell volumes of the inclusion before and after release from the host diamond (Anzolini *et al.*, 2019) or by comparison to a second, stand-alone reference sample of the inclusion mineral. Using this approach, we present the highest residual pressure ever measured for a breyite-diamond pair, which allows us to constrain the origin and geological implications of this super-deep diamond.

Results

Entrapment pressure of breyite. Single-crystal X-ray diffraction (SCXRD) measurement resulted in the following unit-cell parameters for JU55 inclusion 2 (Fig. 1a, inclusion in the black square): $a = 6.31(3)$ Å, $b = 6.60(1)$ Å, $c = 9.24(3)$ Å, $\alpha = 84.3(2)°$, $\beta = 71.8(3)°$, $\gamma = 77.38(3)°$, and $V = 356(2)$ Å^3. This unit-cell volume was used to calculate the residual pressure (P_{inc}) using the EoSFit7c software (Angel *et al.*, 2014) and the equation of state of breyite published by Anzolini *et al.* (2016). This was possible comparing our unit-cell volume with that of the holotype breyite (Brenker *et al.*, 2021), which was measured using exactly the same instrumental set-up used in this work. The room pressure volume determined in Brenker *et al.* (2021) was 376.72(4) Å^3. Comparing this volume with our volume determination and using the P–V equation of state of breyite (Anzolini *et al.*, 2016), we obtained a residual pressure P_{inc} value of 5.4 ± 0.6 GPa. This is the highest residual pressure ever stored in a diamond existing at Earth's surface in a single-phase breyite inclusion. Using this P_{inc} along with the thermo-elastic properties of breyite (Anzolini *et al.*, 2016), of diamond (Angel *et al.*, 2015) and the EosFit-Pinc software (Angel *et al.*, 2017, 2022), we calculated the so-called "isomekes" (see Supplementary Information), which provide the entrapment pressure (P_{trap}) of the diamond-breyite pair over a temperature range from 1000 to 2000 °C (Table 1). This approach yielded a pressure of formation ranging from ~9 ± 1 GPa (about 270 km depth) at 1000 °C to ~10 ± 1 GPa (310 km depth) at 2000 °C. These pressures are only minimum estimates because the inclusion shows small, optically visible cracks (Fig. 1c). The uncertainty given for P_{trap} only represents an estimation. The minimum and maximum variation of P_{trap} was determined as a function of P_{inc} and its uncertainty (Table 1). The entire range of T–P entrapment conditions of our breyite is plotted in Figure 2 within the phase diagram of the $CaSiO_3$-system. Our calculated T_{trap}–P_{trap} plots in the deepest possible area of the breyite stability field, close to the phase boundary between $CaSi_2O_5$-titanite and larnite (β-Ca_2SiO_4). At ambient mantle temperatures close to 1400–1500 °C, our calculated P_{trap} (Fig. 2) definitively exceeds the breyite T–P stability field. The diamond contains further breyite inclusions [Fig. 1a; at least four colourless inclusions are visible within the largest white rectangle indicated by two groups, 1(1) and 1(2)]; however, the diffraction and micro-Raman data (see Supplementary Information) on such inclusions indicated very low residual pressure P_{inc} likely due to typical pervasive presence of fractures that likely led to a significant pressure release.

Table 1 *T–P* entrapment conditions for breyite in this study. The table reports the T_{trap}–P_{trap} data calculated at P_{inc} = 5.4 ± 0.6 GPa obtained from our X-ray diffraction volume data. These data were used to plot the T_{trap}–P_{trap} area in Figure 2. The uncertainty given for P_{trap} is an estimation given by using the minimum and maximum value of P_{inc} to calculate P_{trap} with the EosFitPinc software (Angel *et al.*, 2017, 2022).

T_{trap} (°C)	P_{trap} (GPa) for P_{inc} = 5.4 ± 0.6 GPa
1000	8.9
1100	9.1
1200	9.2
1300	9.4
1400	9.5
1500	9.7
1600	9.8
1700	9.9
1800	10.1
1900	10.2
2000	10.3

Note: the estimated uncertainty in P_{trap} is ±1 GPa.

Phase identification by optical microscopy. Optical microscopy was used to identify phases which could not be analysed by micro-Raman spectroscopy and X-ray diffraction (see Supplementary Information). Most inclusions were black and small; based on their black colour these inclusions were interpreted to be graphite. Two inclusions showed a bright metallic and typical iridescent blue colour and we interpreted them as two ferropericlases (Fig. 1e, f). Unfortunately, the extremely small size of these two inclusions did not allow us to identify them by X-ray diffraction.

Discussion

An individual breyite inclusion in a super-deep diamond can form in the upper mantle by a variety of mechanisms, as described in Brenker *et al.* (2021). Yet, breyite can also form as the higher-pressure polymorph of Ca-silicate perovskite encapsulated in diamond in the transition zone or lower mantle. Distinguishing between these two crystallisation scenarios is essential to better understand geochemical recycling and mantle convection across the mantle transition zone. With the direct determination of residual pressure by X-ray diffraction in the lab and the elastic geobarometric calculation tools available now for this mineral, as proposed by Anzolini *et al.* (2016, 2018), we can more accurately estimate the minimum pressure of breyite crystallisation at depth. Our results in this study indicate that the single breyite shows extremely high entrapment pressures (Fig. 2). These entrapment pressures are too high for the maximum T–P stability field determined experimentally for breyite and are not physically possible.

The logical explanation is that our breyite was formed originally as $CaSiO_3$-perovskite, likely in the transition zone or in the lower mantle. Two iridescent inclusions, optically identified as ferropericlase but too small to confirm by other methods (Fig. 1e, f), would support this explanation because $CaSiO_3$-perovskite + ferropericlase is a typical assemblage of the lower mantle in presence of bridgmanite and would be stable at least from a minimum depth of 450 km (Liu, 1979). We interpret the absence of bridgmanite as due to the generally poor ability of diamond to capture a complete modal mineral assemblage from its host rock; this is typical in diamond crystallisation. The alternative explanation, *i.e.* our breyite formed as a back transformation from larnite + $CaSi_2O_5$-titanite above 11–12 GPa, can be ruled out because, at least to our knowledge, no *HP*–*HT* experimental evidence exists for larnite + $CaSi_2O_5$-titanite + ferropericlase as a stable assemblage in the upper mantle down to 410 km depth.

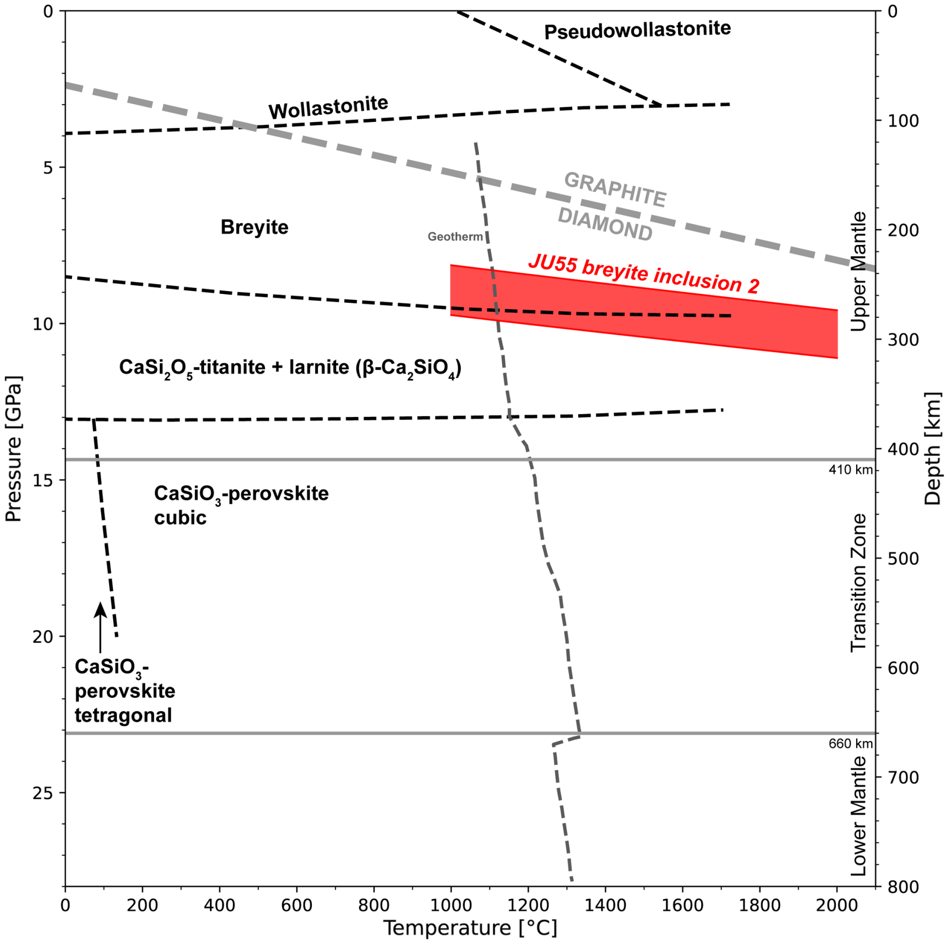

Figure 2 Phase diagram of the $CaSiO_3$ system for inclusion 2 in JU55, where the $CaSiO_3$ phase relations of Sagatova *et al.* (2021) are given as black dashed lines. The graphite-diamond phase boundary is given as a grey dashed line (Day, 2012). The geotherm was taken from Agee (1998). The 410 and 660 km discontinuities are given as grey lines. The entrapment pressures of the breyite inclusion are indicated by the red area.

The ability to use common minerals such as breyite, often found singly in super-deep diamonds, as a reliable pressure indicator contributes greatly to understanding the geology of the mantle transition zone and lower mantle—especially when combined with other inclusions in the same diamond. Important constraints are needed on the fate of subducted slabs, how slabs release fluids at depth, how much fluid is in this region, and even the longstanding question of material transport across the 410 and 660 km seismic discontinuities. For example, the presence of magnesite (see Supplementary Information) in diamond JU55, combined with our geobarometric determinations on breyite, provides direct evidence for the existence of carbonate at lower mantle conditions. Given the link between super-deep diamonds and subducting slabs (*e.g.*, Shirey *et al.*, 2021; Walter *et al.*, 2022), along with constraints from slab thermal modelling and phase equilibria showing the possibility of transporting carbonate to the lower mantle in the carbonated crust of subducting slabs (Walter *et al.*, 2022), we suggest that the breyite *T–P* estimates and magnesite in diamond JU55 are evidence of carbon transport to lower mantle depths.

Acknowledgement

This study was founded by the German Science Foundation DFG (project BR 2015/36-1).

Editor: Francis McCubbin

Additional Information

Supplementary Information accompanies this letter at https://www.geochemicalperspectivesletters.org/article2313.

Cite this letter as: Genzel, P.-T., Pamato, M.G., Novella, D., Santello, L., Lorenzon, S., Shirey, S.B., Pearson, D.G., Nestola, F., Brenker, F.E. (2023) Geobarometric evidence for a LM/TZ origin of $CaSiO_3$ in a sublithospheric diamond. *Geochem. Persp. Let.* 25, 41–45. https://doi.org/10.7185/geochemlet.2313

References

Agee, C.B. (1998) Phase transformation and seismic structure in the upper mantle and transition zone. In: Hemley, R.J. (Ed.) *Ultrahigh-Pressure Mineralogy*. Reviews in Mineralogy 37, Mineralogical Society of America, Washington, D.C., De Gruyter, Berlin/Munich/Boston, 165–204. https://doi.org/10.1515/9781501509179-007

Angel, R.J., Alvaro, M., Gonzalez-Platas, J. (2014) EosFit7c and a Fortran module (library) for equation of state calculations. *Zeitschrift für Kristallographie - Crystalline Materials* 229, 405–419. https://doi.org/10.1515/zkri-2013-1711

Angel, R.J., Alvaro, M., Nestola, F., Mazzucchelli, M.L. (2015) Diamond thermoelastic properties and implications for determining the pressure of formation of diamond-inclusion systems. *Russian Geology and Geophysics* 56, 211–220. https://doi.org/10.1016/j.rgg.2015.01.014

Angel, R.J., Mazzucchelli, M.L., Alvaro, M., Nestola, F. (2017) EosFit-Pinc: A simple GUI for host-inclusion elastic thermobarometry. *American Mineralogist* 102, 1957–1960. https://doi.org/10.2138/am-2017-6190

Angel, R.J., Alvaro, M., Nestola, F. (2022) Crystallographic Methods for Nondestructive Characterization of Mineral Inclusions in Diamonds. *Reviews in Mineralogy and Geochemistry* 88, 257–305. https://doi.org/10.2138/rmg.2022.88.05

Anzolini, C., Angel, R.J., Merlini, M., Derzsi, M., Tokár, K., Milani, S., Krebs, M.Y., Brenker, F.E., Nestola, F., Harris, J.W. (2016) Depth of formation of $CaSiO_3$-walstromite included in super-deep diamonds. *Lithos* 265, 138–147. https://doi.org/10.1016/j.lithos.2016.09.025

Anzolini, C., Prencipe, M., Alvaro, M., Romano, C., Vona, A., Lorenzon, S., Smith, E.M., Brenker, F.E., Nestola, F. (2018) Depth of formation of super-deep diamonds: Raman barometry of $CaSiO_3$-walstromite inclusions. *American Mineralogist* 103, 69–74. https://doi.org/10.2138/am-2018-6184

Anzolini, C., Nestola, F., Mazzucchelli, M.L., Alvaro, M., Nimis, P., Gianese, A., Morganti, S., Marone, F., Campione, M., Hutchison, M.T., Harris, J.W. (2019) Depth of diamond formation obtained from single periclase inclusions. *Geology* 47, 219–222. https://doi.org/10.1130/G45605.1

Brenker, F.E., Vincze, L., Vekemans, B., Nasdala, L., Stachel, T., Vollmer, C., Kersten, M., Somogyi, A., Adams, F., Joswig, W., Harris, J.W. (2005) Detection of a Ca-rich lithology in the Earth's deep (>300 km) convecting mantle. *Earth and Planetary Science Letters* 236, 579–587. https://doi.org/10.1016/j.epsl.2005.05.021

Brenker, F.E., Vollmer, C., Vincze, L., Vekemans, B., Szymanski, A., Janssens, K., Szaloki, I., Nasdala, L., Joswig, W., Kaminsky, F. (2007) Carbonates from the lower part of transition or even the lower mantle. *Earth and Planetary Science Letters* 260, 1–9. https://doi.org/10.1016/j.epsl.2007.02.038

Brenker, F.E., Nestola, F., Brenker, L., Peruzzo, L., Harris, J.W. (2021) Origin, properties, and structure of breyite: The second most abundant mineral inclusion in super-deep diamonds. *American Mineralogist* 106, 38–43. https://doi.org/10.2138/am-2020-7513

Bulanova, G.P., Walter, M.J., Smith, C.B., Kohn, S.C., Armstrong, L.S., Blundy, J., Gobbo, L. (2010) Mineral inclusions in sublithospheric diamonds from Collier 4 kimberlite pipe, Juina, Brazil: subducted protoliths, carbonated melts and primary kimberlite magmatism. *Contributions to Mineralogy and Petrology* 160, 489–510. https://doi.org/10.1007/s00410-010-0490-6

Day, H.W. (2012) A revised diamond-graphite transition curve. *American Mineralogist* 97, 52–62. https://doi.org/10.2138/am.2011.3763

Fedoraeva, A.S., Shatskiy, A., Litasov, K.D. (2019) The join $CaCO_3$-$CaSiO_3$ at 6 GPa with implication to Ca-rich lithologies trapped by kimberlitic diamonds. *High Pressure Research* 39, 547–560. https://doi.org/10.1080/08957959.2019.1660325

Harte, B. (2010) Diamond formation in the deep mantle: the record of mineral inclusions and their distribution in relation to mantle dehydration zones. *Mineralogical Magazine* 74, 189–215. https://doi.org/10.1180/minmag.2010.074.2.189

Joswig, W., Stachel, T., Harris, J.W., Baur, W.H., Brey, G.P. (1999) New Ca-silicate inclusions in diamonds — tracers from the lower mantle. *Earth and Planetary Science Letters* 173, 1–6. https://doi.org/10.1016/S0012-821X(99)00210-1

Kaminsky, F. (2012) Mineralogy of the lower mantle: A review of 'super-deep' mineral inclusions in diamond. *Earth-Science Reviews* 110, 127–147. https://doi.org/10.1016/j.earscirev.2011.10.005

Kubo, A., Suzuki, T., Akaogi, M. (1997) High pressure phase equilibria in the system $CaTiO_3$-$CaSiO_3$: stability of perovskite solid solutions. *Physics and Chemistry of Minerals* 24, 488–494. https://doi.org/10.1007/s002690050063

Lui, L.-G. (1979) The high-pressure phase transformations of monticellite and implications for upper mantle mineralogy. *Physics of the Earth and Planetary Interiors* 20, 25–29. https://doi.org/10.1016/0031-9201(79)90101-8

Maeda, F., Ohtani, E., Kamada, S., Sakamaki, T., Hirao, N., Ohishi, Y. (2017) Diamond formation in the deep lower mantle: a high-pressure reaction of $MgCO_3$ and SiO_2. *Scientific Reports* 7, 40602. https://doi.org/10.1038/srep40602

Sagatova, D.N., Shatskiy, A.F., Sagatov, N.E., Litasov, K.D. (2021) Phase Relations in $CaSiO_3$ System up to 100 GPa and 2500 K. *Geochemistry International* 59, 791–800. https://doi.org/10.1134/S0016702921080073

Shirey, S.B., Cartigny, P., Frost, D.J., Keshav, S., Nestola, F., Nimis, P., Pearson, D.G., Sobolev, N.V., Walter, M.J. (2013) Diamonds and the Geology of Mantle Carbon. *Reviews in Mineralogy and Geochemistry* 75, 355–421. https://doi.org/10.2138/rmg.2013.75.12

Shirey, S.B., Wagner, L.S., Walter, M.J., Pearson, D.G., van Keken, P.E. (2021) Slab Transport of Fluids to Deep Focus Earthquake Depths—Thermal Modeling Constraints and Evidence From Diamonds. *AGU Advances* 2, e2020AV000304. https://doi.org/10.1029/2020AV000304

Stachel, T. (2001) Diamonds from the asthenosphere and the transition zone. *European Journal of Mineralogy* 13, 883–892. https://doi.org/10.1127/0935-1221/2001/0013-0883

Stachel, T., Harris, J.W. (2008) The origin of cratonic diamonds — Constraints from mineral inclusions. *Ore Geology Reviews* 34, 5–32. https://doi.org/10.1016/j.oregeorev.2007.05.002

Stachel, T., Harris, J.W. (2009) Formation of diamond in the Earth's mantle. *Journal of Physics: Condensed Matter* 21, 364206. http://doi.org/10.1088/0953-8984/21/36/364206

Thomson, A.R., Walter, M.J., Kohn, S.C., Brooker, R.A. (2016) Slab melting as a barrier to deep carbon subduction. *Nature* 529, 76–79. https://doi.org/10.1038/nature16174

Walter, M.J., Thomson, A.R., Smith, E.M. (2022) Geochemistry of Silicate and Oxide Inclusions in Sublithospheric Diamonds. *Reviews in Mineralogy and Geochemistry* 88, 393–450. https://doi.org/10.2138/rmg.2022.88.07

Woodland, A.B., Girnis, A.V., Bulatov, V.K., Brey, G.P., Höfer, H.E. (2020) Breyite inclusions in diamond: experimental evidence for possible dual origin. *European Journal of Mineralogy* 32, 171–185. https://doi.org/10.5194/ejm-32-171-2020

Zedgenizov, D.A., Ragozin, A.L., Kalinina, V.V., Kagi, H. (2016) The mineralogy of Ca-rich inclusions in sublithospheric diamonds. *Geochemistry International* 54, 890–900. https://doi.org/10.1134/S0016702916100116

Geochemical Perspectives Letters

Geobarometric evidence for a LM/TZ origin $CaSiO_3$ in a sublithospheric diamond

P.-T. Genzel, M.G. Pamato, D. Novella, L. Santello, S. Lorenzon, S.B. Shirey, D.G. Pearson, F. Nestola, F.E. Brenker

Supplementary Information

The Supplementary Information includes:

- Material and Methods
- Figures S-1 to S-3
- Supplementary Information References

Material and Methods

Sample. The investigated diamond, Juina São Luiz 05192014 1a 055 (hereafter JU55; Fig. 1a, b), comes from the alluvial diamond deposit of the São Luiz River, in the Juina Area, Mato Grosso State, Brazil. JU55 is a 0.16 carat diamond with dimensions of approximately 4.5 × 3 × 1.5 mm^3. In this study, we performed a non-destructive analysis of a single phase breyite inclusion (named inclusion 2) with a maximum dimension of ~120 µm, which is still enclosed in its host diamond (Fig. 1a, black square in Fig. 1c) by single-crystal X-ray diffraction (hereafter SCXRD). Further inclusions of JU55 were analysed by micro-Raman spectroscopy (hereafter MRS) and optical microscopy.

In situ single-crystal X-ray diffraction. The X-ray data were collected using a Rigaku Oxford Diffraction SuperNova diffractometer equipped with a Mova X-ray micro-source and a Dectris Pilatus 200 K area detector at the Department of Geosciences of the University of Padova, Italy. For the measurements, a Mo$K\alpha$ micro-X-ray source operating at 50 kV and 0.8 mA with a radiation wavelength of 0.71073 Å was used. The detector-to-sample distance was set to 68 mm. The size of the beam spot is about 120 µm. Before the actual measurement, several scans at different phi-angles were performed to test the precise position of the inclusion under the X-ray beam. Data reduction was performed using the CrysAlis^{Pro} software (Rigaku Oxford Diffraction).

Micro-Raman spectroscopy. *In situ* MRS was performed at the Department of Geosciences of the University of Padova, Italy, using a WITec alpha300 R Raman Imaging Microscope equipped with a green laser (532 nm). The single spectra were collected using a 50× long working distance objective. The Raman system was set with 300 lines/mm grating. For every inclusion, two spectra were collected with two different frequency ranges. The first spectrum was collected over a frequency range extending from 0 to 4000 cm^{-1} and the second from 200 to 1250 cm^{-1}. Spectra collection over a shorter frequency range was performed to obtain higher intensities for the single inclusion Raman bands, as the intensity of the first order diamond band located at 1332 cm^{-1} is much higher than the intensity for the Raman bands of the various inclusions trapped inside the diamond. Each spectrum was accumulated 10 times using an integration time of 10 s; at the end of the acquisition the spectra were merged. The Raman instrument was calibrated with a silicon plate for intensity and correct position of the 520 cm^{-1} silica band. Background correction, with a linear function and Lorentzian fitting were done using the open-source software Fityk (Wojdyr, 2010).

Optical microscopy. Optical microscopy was performed with a Keyence digital microscope VHX-6000 at the Geoscience Institute, Goethe University Frankfurt. Two objectives with magnifications from 20× to 200× and from 200× to 2000× were used to identify the mineral inclusions in JU55.

Breyite inclusions in groups 1 and 2. Beyond the inclusion 2 in Figure 1a within the black square, the same figure shows within the largest white rectangle two further groups of inclusions, which are here called group 1(1) and group 1(2). Single-crystal X-ray diffraction on these two groups of inclusions identified them as further breyites. The unit-cell parameters and volumes of these four breyite are:

Group 1
1(1a) a = 6.662(9) Å, b = 6.571(13) Å, c = 9.165(15) Å, α = 83.6(2)°, β = 69.8(1)°, γ = 77.1(2)°, V = 364.6(10) $Å^3$
1(1b) a = 6.631(10) Å, b = 6.627(11) Å, c = 9.185(16) Å, α = 84.2(2)°, β = 69.7(2)°, γ = 77.3(2)°, V = 369.1(9) $Å^3$

Group 2
1(2a) a = 6.641(14) Å, b = 6.651(9) Å, c = 9.267(17) Å, α = 69.9(1)°, β = 84.4(2)°, γ = 77.7(1)°, V = 375(1) $Å^3$
1(2b) a = 6.608(13) Å, b = 6.614(19) Å, c = 9.25(2) Å, α = 69.8(2)°, β = 83.8(2)°, γ = 76.7(2)°, V = 369(2) $Å^3$

The volumes of these four inclusions provided residual pressures P_{inc} much lower than that found for inclusion 2; in detail:

Inclusion 1(1a), P_{inc} = 2.982 GPa
Inclusion 1(1b), P_{inc} = 1.818 GPa
Inclusion 1(2a), P_{inc} = 0.394 GPa
Inclusion 1(2b), P_{inc} = 1.843 GPa

The simultaneous presence of inclusions of the same mineral showing different residual pressures is quite common in super-deep diamonds (Anzolini *et al.*, 2016). This is mainly due to the common fractures present in super-deep diamonds, which cause a pressure release. In these cases, the calculation of the pressure of formation is often useless as it will only represent a minimum pressure.

Inclusion phase identification by Raman spectroscopy. *In situ* micro-Raman analyses on inclusion 13 resulted to be magnesite (Fig. S-1), while for inclusion 9 they resulted to be the two coexisting TiO_2 polymorphs rutile and anatase (Fig. S-2). Micro-Raman spectroscopy was also useful to confirm the breyite identification carried out by X-ray diffraction for inclusions of groups 1 and 2 (see Fig. 1a within the white rectangle). In detail, we collected a few Raman spectra, which were compared with the Raman spectrum of breyite holotype in Brenker *et al*. (2021). In Figure S-3, we plotted two typical Raman spectra of breyite found for groups 1 and 2.

The concept of the isomeke. As well described in the extensive review by Angel *et al.* (2022), in the exact moment when a diamond entraps an inclusion, they are at the same pressure and temperature; under these conditions, the inclusion completely fills the void within the diamond, which means that the void inside the diamond and the inclusion must occupy the same volume. Once the entrapment is completed and the diamond moves, if "*the pressure and temperature change in such a way that the natural expansion and contraction of a free crystal of the inclusion exactly matches that of the host diamond, the inclusion will continue to exactly fit the void space in the diamond without* *the application of any additional stress*" (Angel *et al.*, 2022). The pressure–temperature values lie on a line that is called "isomeke" (Rosenfeld and Chase, 1961; Adams *et al.*, 1975), which is defined by the difference in the thermoelastic properties (volume thermal expansion and compressibility) of diamond and its inclusion. Thus, if we have available an equation of state for the host-inclusion system, we can calculate an isomeke and this is what we have done in this work using the equation of state of breyite (Anzolini *et al.*, 2016) and that of diamond (Angel *et al.*, 2015). In Figure 2, we have plotted a coloured area which is constituted by a series of isomekes covering all *P*-*T* values within the experimental uncertainty from our unit-cell volume calculation (and thus from our P_{inc}).

Supplementary Figures

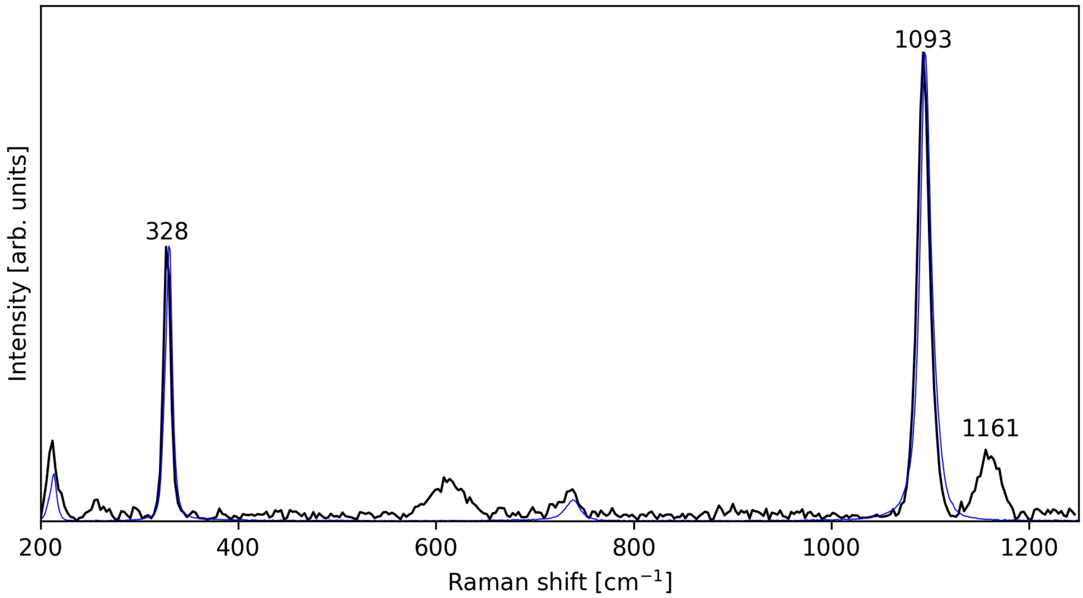

Figure S-1 Raman spectrum of magnesite (inclusion 13 in Fig. 1a) compared to the magnesite reference R040114 from the RRUFF Raman database (Lafuente *et al.*, 2016).

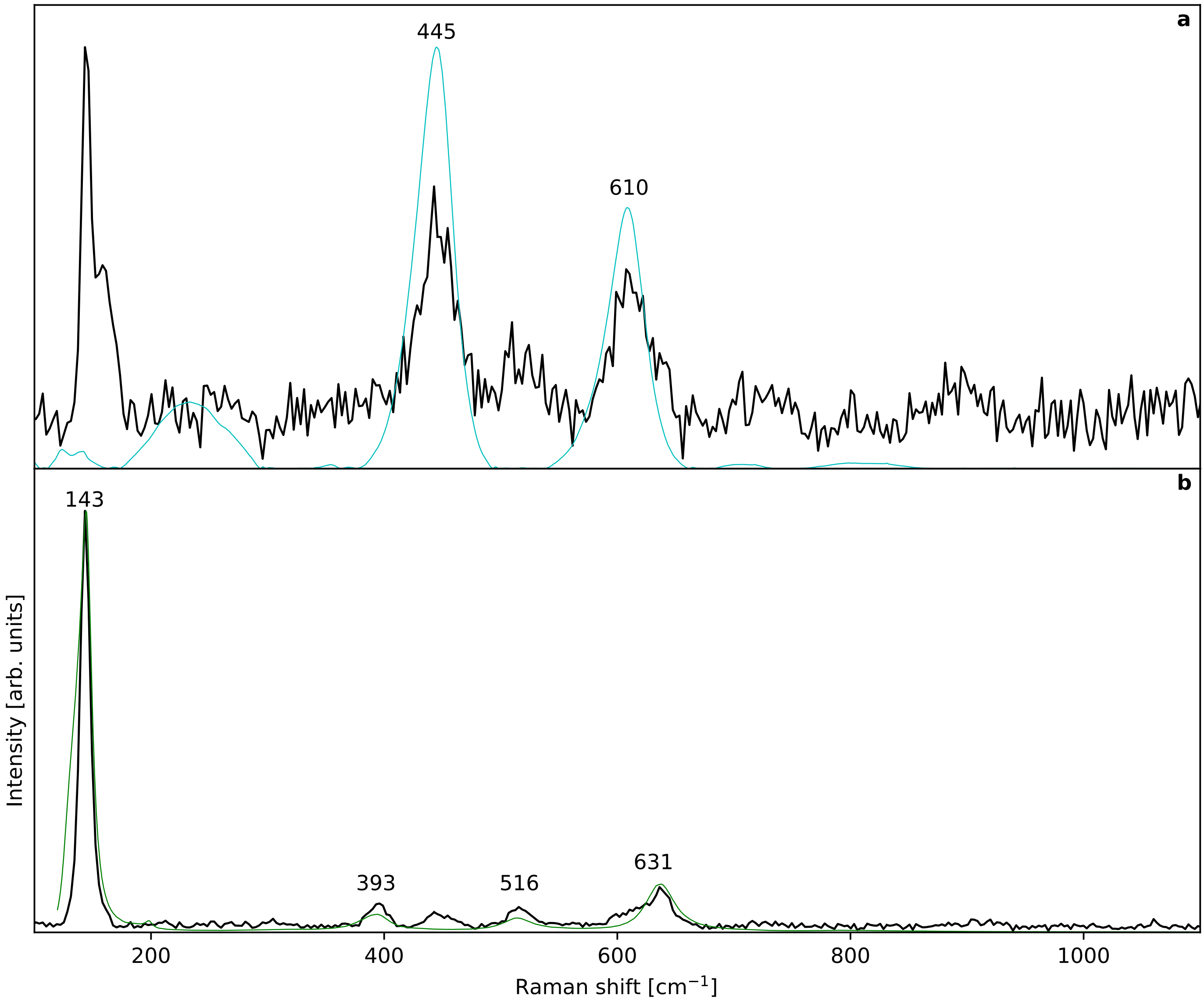

Figure S-2 Raman spectra of rutile and anatase (inclusion 9 in Fig. 1a) compared to the rutile reference R060493 and anatase reference R070582 from RRUFF Raman database (Lafuente *et al.*, 2016). Our data are plotted in black in both **(a)** and **(b)**.

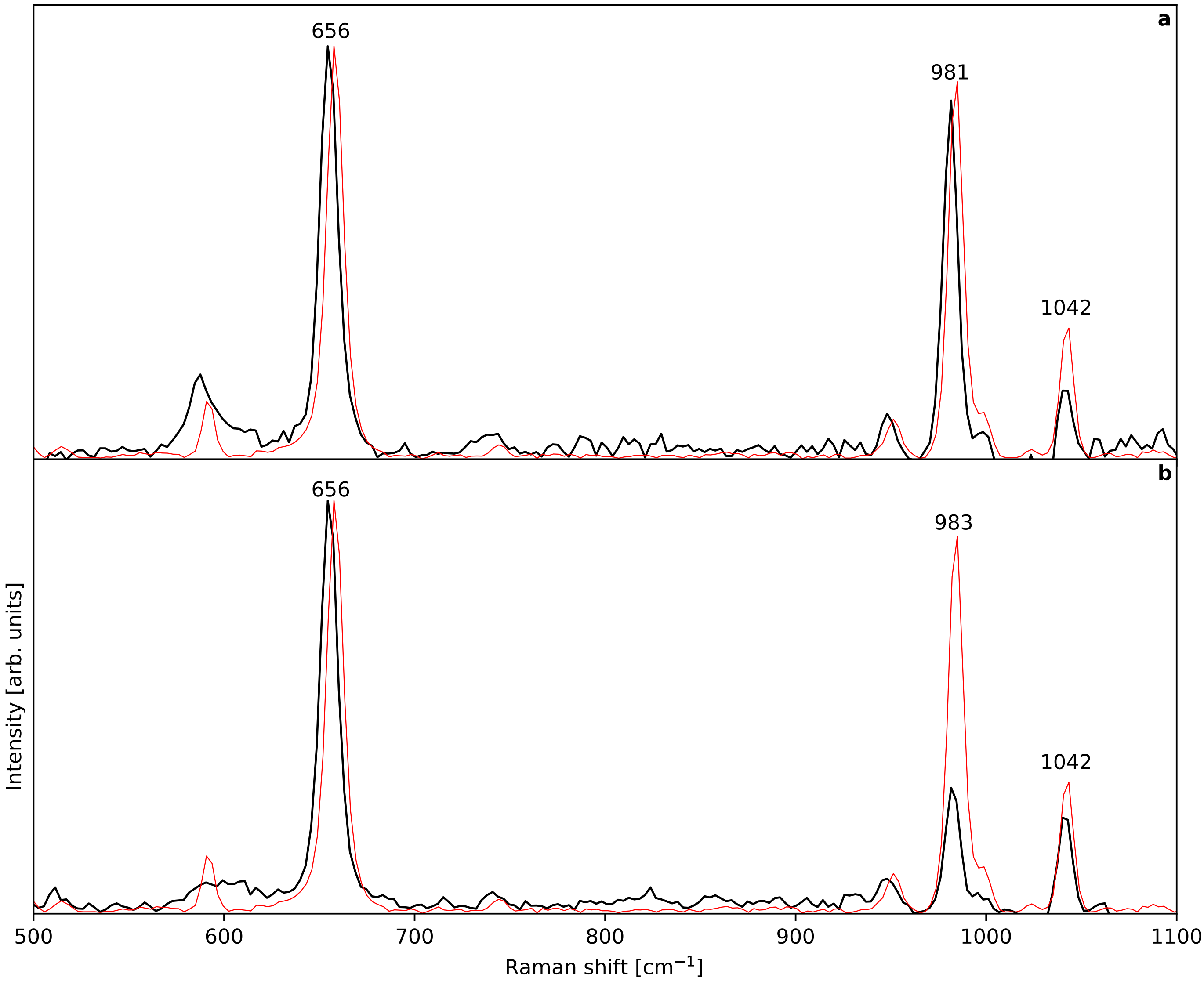

Figure S-3 Raman spectra of two breyites [inclusions from groups 1(1) and 1(2) in Fig. 1a] compared to the Raman spectrum of the holotype breyite by Brenker *et al*. (2021). In detail, in **(a)** we plotted a breyite from group 1(1) and in **(b)** a breyite from group 1(2). The red spectrum is the breyite holotype from Brenker *et al*. (2021) in both **(a)** and **(b)**, whereas our data are plotted in black.

Supplementary Information References

Adams, H.G., Cohen, L.H., Rosenfeld, J.L. (1975) Solid inclusion piezothermometry I: Comparison dilatometry. *American Mineralogist* 60, 574–583. https://pubs.geoscienceworld.org/msa/ammin/article-abstract/60/9-10/944/543164/Solid-inclusion-piezothermometry-I-Comparison?redirectedFrom=fulltext

Angel, R.J., Alvaro, M., Nestola, F., Mazzucchelli, M.L. (2015) Diamond thermoelastic properties and implications for determining the pressure of formation of diamond–inclusion systems. *Russian Geology and Geophysics* 56, 211–220. https://doi.org/10.1016/j.rgg.2015.01.014

Angel, R.J., Alvaro, M., Nestola, F. (2022) Crystallographic Methods for Non-destructive Characterization of Mineral Inclusions in Diamonds. *Reviews in Mineralogy and Geochemistry* 88, 257–305. https://doi.org/10.2138/rmg.2022.88.05

Anzolini, C., Angel, R.J., Merlini, M., Derzsi, M., Tokár, K., Milani, S., Krebs, M.Y., Brenker, F.E., Nestola, F., Harris, J.W. (2016) Depth of formation of $CaSiO_3$-walstromite included in super-deep diamonds. *Lithos* 265, 138–147. https://doi.org/10.1016/j.lithos.2016.09.025

Brenker, F.E., Nestola, F., Brenker, L., Peruzzo, L., Harris, J.W. (2021) Origin, properties, and structure of breyite: The second most abundant mineral inclusion in super-deep diamonds. *American Mineralogist* 106, 38–43. https://doi.org/10.2138/am-2020-7513

Lafuente, B., Downs, R.T., Yang, H., Stone, N. (2016) 1. The power of databases: the RRUFF project. In: Armbruster, T., Danisi, R.M. (Eds.) *Highlights in Mineralogical Crystallography*. De Gruyter, Berlin, 1–30. https://doi.org/10.1515/9783110417104-003

Rosenfeld, J.L., Chase, A.B. (1961) Pressure and temperature of crystallization from elastic effects around solid inclusion minerals? *American Journal of Science* 259, 519–541. https://doi.org/10.2475/ajs.259.7.519

Wojdyr, M. (2010) *Fityk*: a general-purpose peak fitting program. *Journal of Applied Crystallography* 43, 1126–1128. https://doi.org/10.1107/S0021889810030499